Research Article Vol. 33, No. 2 / 27 Jan 2025 / Optics Express 1680
Optics EXPRESS

Realization of a 4 kHz, large energy single-frequency ns optical parametric oscillator by suppressing optical parametric generation

XUECHEN CAO,[1,†] DONGLIN CHENG,[1,†] YANAN CHEN,[1] PIXIAN JIN,[1,2] JING SU,[1,2,4] FANG LI,[3,5] AND HUADONG LU[1,2,6]

[1]State Key Laboratory of Quantum Optics and Quantum Optics Devices, Institute of Opto-Electronics, Shanxi University, Taiyuan 030006, China
[2]Collaborative Innovation Center of Extreme Optics, Shanxi University, Taiyuan 030006, China
[3]Shanxi Bethune Hospital, Shanxi Academy of Medical Sciences, Third Hospital of Shanxi Medical University, Tongji Shanxi Hospital, Taiyuan 030032, China
[4]jingsu@sxu.edu.cn
[5]lifang@sxmu.edu.cn
[6]luhuadong@sxu.edu.cn
[†]The authors contributed equally to this work.

Abstract: Large energy single-frequency nanosecond (ns) near-infrared light source is an essential device in the field of the remote chemical analysis based on the laser-induced breakdown spectroscopy (LIBS). In this paper, a large energy single-frequency ns 824 nm light source with high repetition rate is presented, which is generated from a seed-injection locked optical parametric oscillator (OPO). By optimizing the spot radius of the pump laser and the mode-matching between the pump laser and signal light, the optical parametric generation (OPG) process is effectively eliminated. On this basis, with the assistance of the seed-injection locking, a single-frequency 4 kHz ns 824 nm light source with an output pulse energy and a spectral width of 3.39 mJ and 32.42 MHz is obtained. For the best of our knowledge, it is the largest energy for the single-frequency ns near-infrared light source with the repetition rate of kHz level.

© 2025 Optica Publishing Group under the terms of the Optica Open Access Publishing Agreement

1. Introduction

Near-infrared nanosecond (ns) single-frequency lasers are widely applied in lots of fields including laser spectroscopy, precision measurements, bio-detection and so on since their output laser wavelengths lie on the excellent absorption and penetration of many substances including biological tissues, atmospheric air and chemical elements. Especially, for the remote chemical analysis based on the laser-induced breakdown spectroscopy (LIBS), the intensity of the spectral signals at high energy density can be effectively enhanced by increasing the pulse duration and energy of the laser to the 10 ns and mJ levels, respectively. Meanwhile, the narrowing of the spectral width will be facilitated to improve the signal-noise rate (SNR) and repeatability of the signal [1].

Up to now, Ti:sapphire and alexandrite crystals can generate the near-infrared lasers, but their severe thermal effect because of the high pump rate limit the output power and destroy the beam quality of the achieved lasers [2,3]. Dye media can also be used to generate the near-infrared laser sometimes, but their toxicity is undesired for many researchers [4]. By contrast, 532 nm laser pumped LiB_3O_5 (LBO) optical parametric oscillator (OPO) has become more and more popular candidate to generate the near-infrared laser owing to its high efficiency and ignorable thermal effect. In 2005, Li et al. reported a ns 860 nm laser with a maximum average power of 18 W by employing a OPO consist of two concave mirrors [5]. However, the spectral width of the

#547348 https://doi.org/10.1364/OE.547348
Journal © 2025 Received 7 Nov 2024; revised 25 Dec 2024; accepted 27 Dec 2024; published 13 Jan 2025

Optics EXPRESS

achieved signal light was as wide as 3.0 nm because of the acceptance bandwidth of 1514.9 GHz for the adopted 60 mm LBO crystal at the wavelength of the signal light. In order to narrow the light spectral width, some mode-selective elements including Fabry-Perot (F-P) etalon, grating and so on were inserted into the resonator to increase the loss difference between the main and side modes [6,7]. Although the spectral width of the signal light can be narrowed to a few hundred MHz, it is still a certain gap with spectral width of the Fourier transform limit (FTL). Moreover, the output power and optical conversion efficiency of the OPO is limited to low level since the optical parametric process is free of the mode competition mechanism and the gain of side modes is not transferred to the main mode. Another method to narrow the spectral width is seed-injection locking which is achieved by employing a continuous-wave (CW) single-frequency laser as the seed light [8]. In recent years, our group has developed two ns 824 nm lasers with an output average power and a repetition rate of over 20 W and 50 kHz, respectively, where the spectral width of the obtained 824 nm lasers were effectively narrowed to near FTL based on the developed pulse-saturated seed-injection locking and pulse-integrated seed-injection automatic locking, respectively [9,10].

However, when the pulse energy of the signal light was further increased by increasing the pulse energy of the incident pump laser, the OPO process will be easily accompanied by an optical parametric generation (OPG). In this case, the longitudinal-modes chosen by the OPO resonator are mixed into the continuous spectrum generated by the OPG process. As a result, the energy of the achieved signal light is distributed across different longitudinal-modes. Even if the mode-selective elements or seed-injection locking are employed in the experiment, the OPG can not be effectively suppressed. To solve this problem, in this paper, we present a method to attain a large energy single-frequency ns OPO by suppressing OPG, which is realized by optimizing the pump size and mode-matching between the pump laser and resonator based on the designed variable focus beam expander (VFBE) and equivalent confocal L-shaped OPO. At last, a 4 kHz single-frequency ns 824 nm light source with the output pulse energy of 3.39 mJ successfully is obtained under the incident 532 nm pump laser energy of 9.88 mJ. The optical conversion is up-to 34.31%. The spectral width is narrowed from 2.52 nm in the free-running to 32.42 MHz through employing seed-injection locking.

2. Theoretical analysis

When an OPO depicted in Fig. 1 is pumped by a pulsed laser with large single-pulse energy, the signal and idler light leaked from the OPO will be accompanied by a continuous spectrum generated by the OPG. Moreover, even if the mode-selective elements or seed-injection locking are employed in the experiment, the OPG can't be effectively suppressed because the OPG is free of the OPO resonator. Figure 2 depicts the superimposition results of OPO and OPG. It is clear that the discrete spectrum of OPO and the continuous spectrum of OPG will be superimposed when the OPG is generated, and the influence of the OPG on the achieved spectrum purity is not ignored, although the seed-injection locking is employed. On the contrary, once the OPG can be effectively eliminated, a single-frequency pulsed laser can be easily obtained depending on the seed-injection locking.

In order for this goal, it is found that optimizing the spot radius of the pump laser provides a way to effectively suppress the OPG. The pumping threshold of the OPO and OPG can be expressed as [11,12],

$$\begin{cases} E_{\mathrm{th,OPG}} = \dfrac{\pi\omega_0^2\tau}{2\kappa l^2}\operatorname{arccosh}^2\sqrt{P(l)/P(0)} \\ E_{\mathrm{th,OPO}} = \dfrac{2.25\pi\omega_0^2\tau_{\mathrm{e}}}{2\kappa l^2 g_s(1+\gamma)^2}\left(\dfrac{33L}{2\tau_{\mathrm{e}}c} + 2\alpha l + \ln\dfrac{1}{\sqrt{R}} + \ln 4\right)^2 \end{cases}, \tag{1}$$

Optics EXPRESS

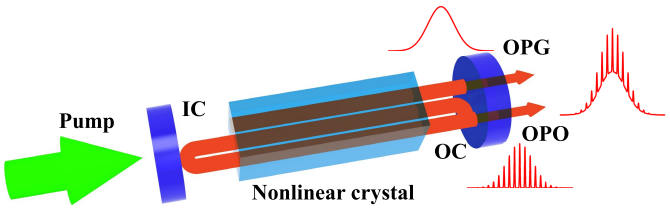


Fig. 1. Schematic diagram of the OPO.

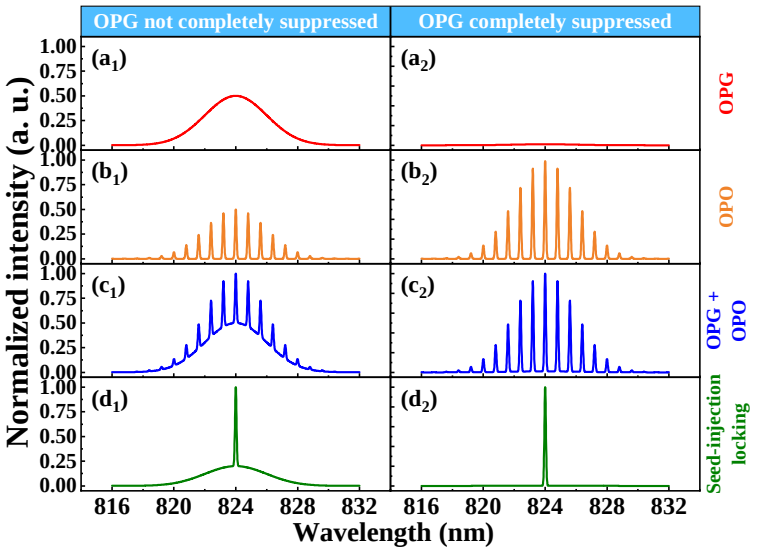


Fig. 2. Schematic diagram of spectral superposition of OPO and OPG.

and

$$\kappa = \frac{8d_{\text{eff}}^2\pi^2}{c\varepsilon_0\lambda_s\lambda_i n_p n_s n_i}. \tag{2}$$

where, c and ε_0 are the speed of light in vacuum and dielectric constant of vacuum, respectively, L is the cavity length of OPO, λ_s and λ_i are the wavelengths of the signal and idler light, respectively, n_p, n_s and n_i are the refractive indices of the nonlinear crystal for the pump, signal and idler wavelengths, respectively. d_{eff}, l and α are the effective nonlinear coefficient, length and absorption coefficient of the nonlinear crystal, respectively, ω_0 and τ are the spot radius and pulse width of the pump laser, which is determined by the full width at half maximum (FWHM) of the spot and pulse duration, respectively. And τ_e is $1/e^2$ intensity halfwidth of the pump pulse. $P(0)$ is the vacuum noise, generally takes a value of 10^{-10} W, and $P(l)$ is the peak power when the signal light of the OPG reaches the threshold, generally valued at 1 μW. g_s is the signal spatial mode coupling coefficient defined by $g_s = (\omega_0^2)/(\omega_0^2 + \omega_s^2)$, where ω_s is the cavity mode radius of the signal light at the crystal. γ is the ratio of backward to forward pump field amplitude inside the crystal, and R is the reflectivity of the output coupler at signal light. According to Eq. (1) and parameters of OPO resonant and LBO crystal in the experiment, the calculated pump threshold can be obtained, which is depicted in Fig. 3(a). Curves (a_1) and (a_2) are the threshold for OPO and OPG, respectively. At the same time, the damage threshold can also easily be obtained according to the characteristic of the LBO crystal [13], which is illustrated by the curve (a_3) in Fig. 3(a). It is seen that the thresholds of OPO and OPG as well as the damage can increase

Optics EXPRESS

with the increase of the spot radius of the pump laser and the value of OPO is lower than that of the OPG. In other words, for a given pump energy, the OPG can be completely suppressed and only OPO works in the resonator by optimizing the spot radius of the pump laser. However, the larger the spot radius of the pump laser is, the lower the conversion efficiency of the OPO is. Figure 3(b) illustrates the relationship between the conversion efficiency of the OPO and the spot radius of the pump laser for different incident pump energy [14]. It is clear that the optimal spot radius is 396 μm for the incident pump energy of 9.88 mJ, as shown by the point A in Fig. 3(a), where the OPG can be just completely eliminated and the conversion efficiency is 38.1%, which is close to the theoretical maximum of 45.8%.

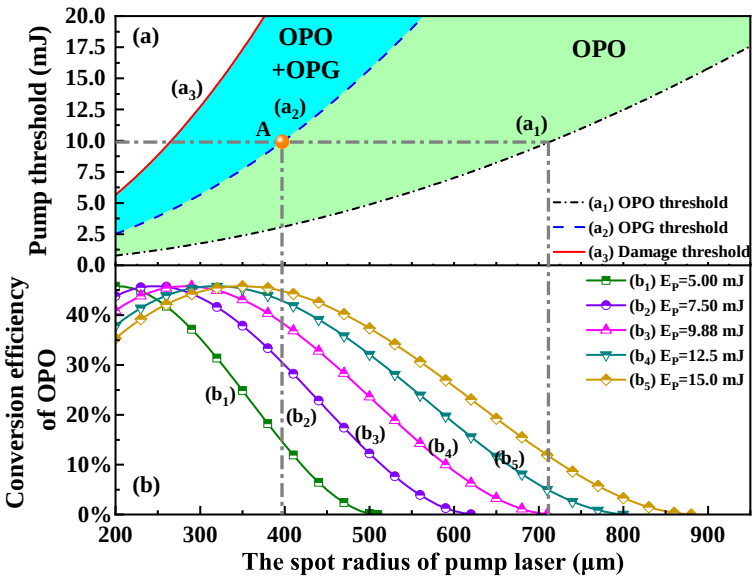


Fig. 3. (a) The relationship between the threshold for the OPO, OPG, and LBO crystal with the spot radius of the pump laser, and (b) The relationship between the conversion efficiency of OPO with pump spot radius at different pump energy.

3. Experimental setup

In order to investigate the influence of the pump size on the OPG suppression, the experimental setup illustrated in Fig. 4 was built. The pump source was a home-made pulsed 532 nm laser with a repetition rate and pulse width of 4 kHz and 15 ns, respectively, and the τ_e was 20 ns. The single-pulse energy was up-to 9.88 mJ. In order to prevent the reflected laser from damaging the pump source, an optical isolator (OI_1) was placed between the pump source and the OPO resonator. Before the pump laser was injected into the resonator of the OPO, a half-wave-plate (HWP) was employed to align the polarization of the incident pump laser, and a VFBE consisted of three lenses (f_1, f_2 and f_3) was utilized to transform the beam size of the pump laser, which was illustrated in Fig. 5(a). The lenses f_1 and f_3 were two concave lenses with focal lengths of −100 and −50 mm, respectively, and the lens f_2 was a convex lens with a focal length of 80 mm. From Fig. 5(b), the spot radius of the pump laser can be continuously changed from 200 μm to 800 μm only through varying the distance l_1 between f_1 and f_2 as well as the distance l_2 between f_2 and f_3, respectively. At the same time, in order to continuously change the cavity mode size of the OPO, an equivalent confocal L-shaped resonator consisting of two planar mirrors (M_2 and M_3), a lens (f_4) and a flat-concave mirror (M_4) with a cavity length of 250 mm was designed and built, which

Optics EXPRESS

was illustrated in Fig. 5(c). As the input coupler, M_2 was coated with an antireflective (AR) film for 532 nm and 1501 nm and a high reflective (HR) film for 824 nm. M_3 was a planar mirror with the incident angle of 45°. In order to filter out the generated idler light in time to avoid the inverse conversion process and realize the double-pass pump of the OPO, it was also coated with an AR film for 532 nm and 1501 nm and an HR film for 824 nm. The flat-concave M_4 with a curvature radius of −50 mm acted as the output coupler and was coated with a partial transmission of 50% for 824 nm. The lens f_4 was inserted into the resonator to achieve an equivalent confocal cavity. When the focal length of f_4 was changed from 80 mm to 130 mm, the spot radius at the position of M_2 can vary from 260 μm to 460 μm after the distance l_4 between f_4 and M_5 was finely matched, as shown in Fig. 5(d). A high-quality ($\alpha \approx 0$) type-I non-critical phase-matching LBO crystal with the size of $3 \times 3 \times 50$ mm^3 was employed to as the OPO medium and placed between M_2 and M_3. To reduce the reflection loss, both front and rear end-faces were coated with AR film for 532 nm, 824 nm and 1501 nm. In addition, M_5 was used to reflect the residual pump laser back to LBO to implement the double-pass pumping.

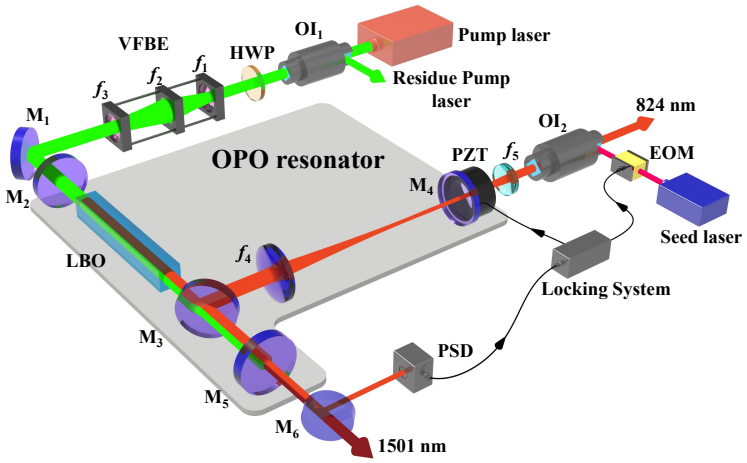


Fig. 4. Experimental configuration of seed injection-locked OPO (M_1 is a beamsplitter and is coated with an HR film for 532 nm and an AR film for 1501 nm, and M_6 is coated with an HR film for 824 nm and an AR film for 1501 nm).

In order to narrow the spectral width of the signal light and obtain a single-frequency 824 nm light, a home-made single-frequency CW tunable Ti:sapphire laser with the spectral width of 350 kHz was employed as the seed laser [15]. The single-frequency 824 nm laser was injected into the OPO resonator from M_4 via an electro-optic modulator (EOM) as well as an optical isolator (OI_2). To achieve impedance matching with the resonator, a lens f_5 was used to shape the spot of the seed laser. The leaked 824 nm laser from M_5 was separated by M_6 and injected into the pulse-saturated detector (PSD) to obtain the error signal. Finally, the error signal was injected into the locking system to attain a feedback signal and loaded on the piezoelectric transducer (PZT) to realize the seed laser locking.

Optics EXPRESS

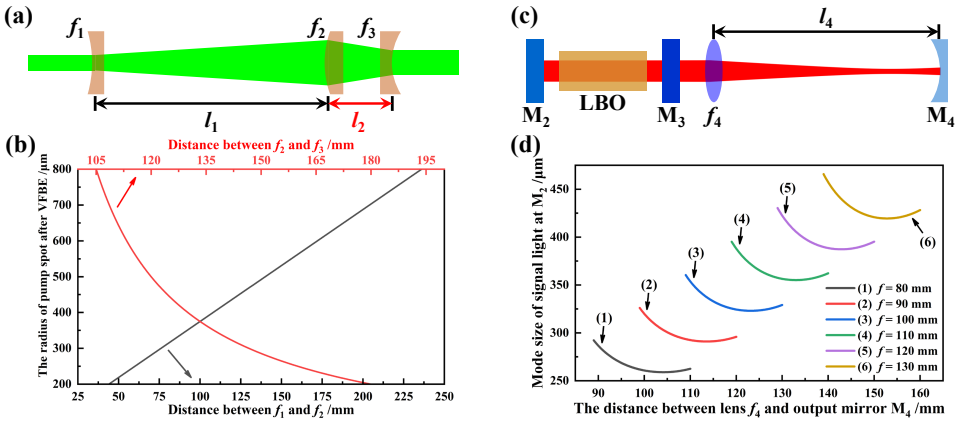


Fig. 5. (a) Schematic of the VFBE and the Beam evolument; (b) Distance between lenses (l_1 and l_2) versus spot radius of pumped laser after VFBE; (c) Schematic of the equivalent SR-OPO cavity and intracavity mode variation; (d) At different focal lengths of f_4, the mode size of signal light at M_2 versus the distance between the lens f_4 and the M_4.

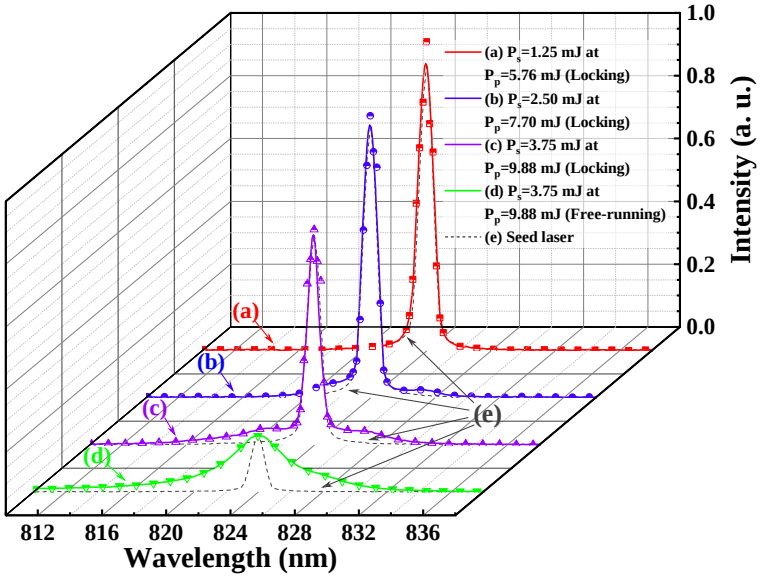


Fig. 6. Spectra of signal light at pump spot radius of 275 μm.

Optics EXPRESS

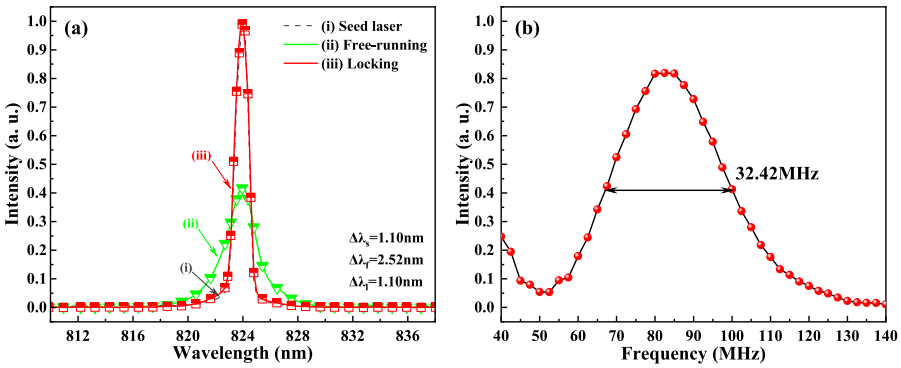


Fig. 7. Spectra of signal light measured by (a) spectrometer and (b) frequency-beating with the seed laser, respectively, at pump spot radius of 396 μm.

4. Experimental results

In the experiment, by scanning the temperature of the LBO crystal to 122.4 °C, the wavelengths of the signal and idler lights were tuned to 824 nm and 1501 nm, respectively. The spot radius of the pump laser was changed by the designed VFBE and the mode-matching ($\omega_0/\omega_s = \sqrt{\lambda_P/\lambda_S}$) between the cavity mode at the LBO crystal and pump laser was achieved by replacing f_4 with different focal length and varying the length of l_4, respectively. The output optical spectrum was firstly monitored by a spectrometer (Maya2000 Pro, Ocean Optics) with an optical resolution of 1.10 nm. Figure 6 and Fig. 7(a) depicted the spectra of the signal light for different pump spot radii before and after the seed injection locking was employed. When the spot radius of the pump laser was 275 μm in Fig. 6, the output energy of the pulse signal light was up-to 3.75 mJ under the pump energy of 9.88 mJ, but the spectral width of the achieved signal light was as wide as 4.60 nm because the pump energy was larger than the OPG threshold of 4.75 mJ, which meant that signal light generated from the OPO was accompanied by the OPG processes, where the spectrum width was determined by measuring the FWHM of the achieved optical spectral signal. In this case, if a 300 mW single-frequency CW 824 nm laser output from a Ti:sapphire laser acted as the seed light and was injected into the resonator, the spectral width of the signal light was narrowed to 1.10 nm, but two distinct small hills were observed on either side of the central wavelength of 824 nm, which revealed that the effect of the seed-injection locking on the linewidth narrowing was very limited once the OPG is generated in the experiment. At this time, when the pump energy was reduced from 9.88 mJ to 7.70 mJ and 5.76 mJ, respectively, the amplitudes of two small hills dramatically became lower and further diminished, but the energy of the 824 nm laser decreased from 3.75 mJ to 2.50 mJ and 1.25 mJ, respectively. It was clear that it is impossible to obtain a large energy single-frequency seed-injection locked OPO only depending on reduction of the pump spot radius.

However, when the pump spot radius was enlarged to 396 μm corresponding to the calculated OPG threshold, the achieved spectral width of the signal light was effectively narrowed to 2.52 nm before the seed laser was injected into the resonator, as shown in Fig. 7(a). Especially, the spectral width was narrowed to 1.10 nm with the assistance of the seed injection locking, which is equal to that of the injected seed source. It is clear from Fig. 6 and Fig. 7(a) that the single-frequency pulse 824 nm laser can be attained with the assistance of injection locking, only if the OPG process can be completely eliminated. The achieved maximum output energy of the pulsed 824 nm laser was 3.39 mJ, and the optical conversion was up-to 34.31%. The experimental results were well consistent with the theoretical analysis. Then, the real spectral

Optics EXPRESS

width of the signal light was measured by frequency-beating of the generated signal light and seed laser, and the spectral width of 32.42 MHz was obtained, which was illustrated in Fig. 7(b).

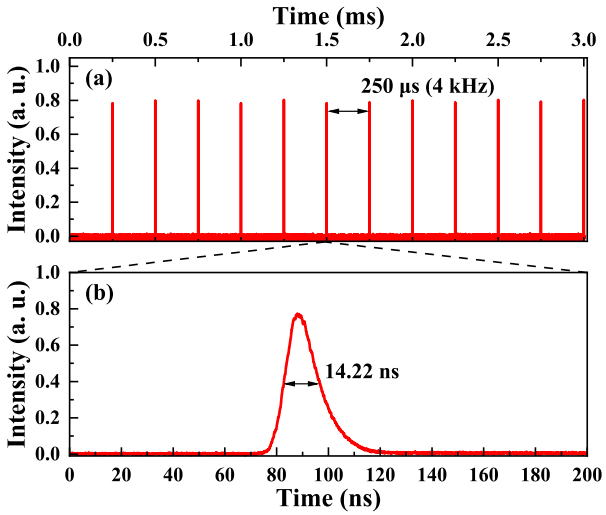


Fig. 8. (a) Pulse sequence, (b) pulse duration of signal light.

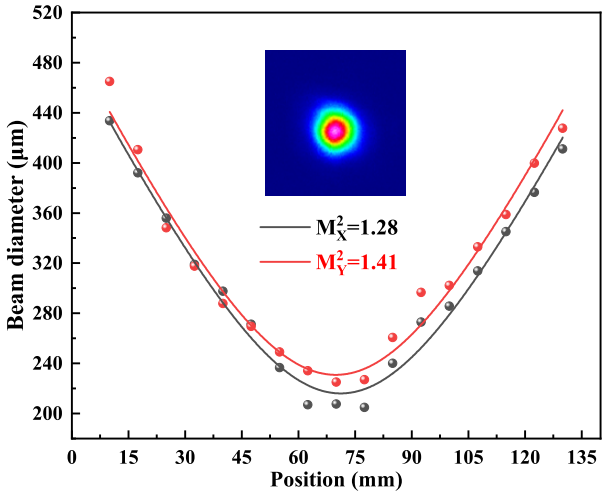


Fig. 9. M^2 factors of signal light.

At last, the pulse sequence and the pulse duration of the signal light was measured by a Si amplified photodetector (PDA10A2, Thorlabs), and the results were shown in Fig. 8(a) and 8(b), which indicated that the repetition rate and pulse width were 4 kHz and 14.22 ns, respectively. At the same time, the beam quality of the signal light were measured by a beam quality analyzer, and the results were shown in Fig. 9, which indicated that the M^2 factors of the beam were 1.28 and 1.47 in the X and Y directions, respectively. The energy fluctuation of signal light was measured by an energy meter (30A-BB-18, Ophir), and the results were shown in Fig. 10, which indicated that the energy fluctuation of signal light was 0.69% (Root-Mean-Square, RMS) in 2 hours.

Optics EXPRESS

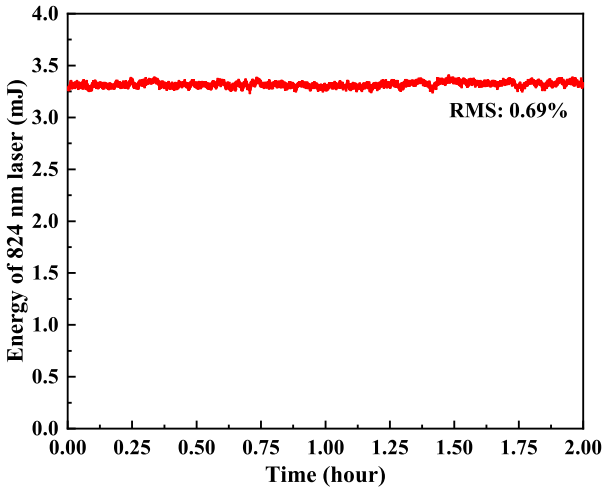


Fig. 10. Energy stability of signal light in 2 h.

5. Conclusion

In a word, we presented a large energy 4 kHz single-frequency ns 824 nm light source, which was generated from a seed-injection locked OPO. Based on the theoretical calculation of the OPO and OPG processes, it was demonstrated that the optimal pump spot size can completely suppress OPG and realize an efficient OPO for a specific pump energy. The pump spot radius and the mode-matching between the pump laser and resonator were optimized based on the designed VFBE and equivalent confocal L-shaped OPO in the experiment. As a result, with the assistance of the seed-injection locking, the output pulse energy and spectral width of the achieved 824 nm light source were 3.39 mJ and 32.42 MHz, respectively. We believe that the presented method can provide a way to realize a large energy and high repetition rate single-frequency ns OPO and the obtained light source can satisfy the requirements of the remote chemical analysis based on the high-SNR LIBS.

Funding. National Natural Science Foundation of China (62027821, 62105192, 62205186); National Key Research and Development Program of China (2022YFC2204003); Scientific and Technological Innovation Programs of Higher Education Institutions in Shanxi; Applied Basic Research Program of Shanxi Province (202103021221004, 202203021212478, 202203021212481); Fund for Shanxi "1331 Project" Key Subjects Construction; Research Project Supported by Shanxi Scholarship Council of China (2022-015); Special fund for Science and Technology Innovation Teams of Shanxi Province (202204051002005); The First Lab - National Innovation Center (Shanxi) Science and Technology Innovation Project; Funding from the National Key Laboratory of Particle Transport and Separation Technology (KWKF-2024-2).

Disclosures. The authors declare no conflicts of interest.

Data availability. Data underlying the results presented in this paper are not publicly available at this time but may be obtained from the authors upon reasonable request.

References

1. R. S. Harmon and G. S. Senesi, "Laser-induced breakdown spectroscopy - a geochemical tool for the 21st century," Appl. Geochem. **128**, 104929 (2021).
2. G. Tawy, J. Wang, and M. J. Damzen, "Pump-induced lensing effects in diode pumped alexandrite lasers," Opt. Express **27**(24), 35865–35883 (2019).
3. S. Cho, J. Jeong, and T. J. Yu, "Jones calculus modeling and analysis of the thermal distortion in a ti:sapphire laser amplifier," Opt. Express **24**(13), 14362–14373 (2016).
4. https://web.archive.org/web/20150221025750/http://www.chemie.unibas.ch/safety/pdf/laser_systems.pdf.
5. H. Q. Li, G. A. Cong, B. Yong, *et al.*, "A 18-w signal average power nanosecond lib_3o_5 optical parametric oscillator around 860 nm and the beam quality," Chin. Phys. Lett. **22**(7), 1694–1697 (2005).

Optics EXPRESS

6. W. R. Bosenberg and D. R. Guyer, "Single-frequency optical parametric oscillator," Appl. Phys. Lett. **61**(4), 387–389 (1992).
7. C. S. Rao, S. Kundu, and A. K. Ray, "Slm operation of a high repetition rate bbo optical parametric oscillator pumped by dpssl at 355 nm," Opt. Laser Technol. **138**, 106878 (2021).
8. J. E. Bjorkholm and H. G. Danielmeyer, "Frequency control of a pulsed optical parametric oscillator by radiation injection," Appl. Phys. Lett. **15**(6), 171–173 (1969).
9. J. L. Qin, J. Q. Song, X. C. Cao, *et al.*, "High-average-power single-longitudinal-mode pulse laser based on a pulse saturation seed-injection locking opo," Opt. Lett. **48**(19), 4973–4976 (2023).
10. J. Q. Song, J. L. Qin, X. C. Cao, *et al.*, "High-average-power single-frequency pulse optical parametric oscillator based on pulse-integrated seed-injection automatic locking," Opt. Lett. **49**(9), 2365–2368 (2024).
11. Y. Q. Lu, J. J. Zheng, Y. L. Lu, *et al.*, "Frequency tuning of optical parametric generator in periodically poled optical superlattice linbo$_3$ by electro-optic effect," Appl. Phys. Lett. **74**(1), 123–125 (1999).
12. S. J. Brosnan and R. L. Byer, "Optical parametric oscillator threshold and linewidth studies," IEEE J. Quantum Electron. **15**(6), 415–431 (1979).
13. https://www.castech.com/product/LBO—Lithium-Triborate-121.html.
14. J. Bjorkholm, "Some effects of spatially nonuniform pumping in pulsed optical parametric oscillators," IEEE J. Quantum Electron. **7**(3), 109–118 (1971).
15. J. Wei, X. C. Cao, P. X. Jin, *et al.*, "Diving angle optimization of brf in a single-frequency continuous-wave wideband tunable titanium:sapphire laser," Opt. Express **29**(5), 6714–6725 (2021).

112.97.57.247 {ts '2025-01-13 13:07:00'}